

## Analysis of Thermal Stress in Fatigue Fracture Specimen using Lock-in Thermography

Won-Tae Kim\*, Man-Yong Choi\*\*, Jung-Hak Park\*\*

\* Major of Bio-mechanical Engineering, Kongju National University, Chungnam, Korea, 340-702

\*\* Safety Measurement Group, Korea Research Institute of Standards and Science, Daejeon, Korea, 305-600

### Abstract

This paper aims to describe the thermal stress analysis using Lock-in thermography as a nondestructive testing(NDT). Applying the method of IR thermographic measurement would significantly reduce the necessary specimens and testing duration. As this technology is based on the thermal elastic effects, it can be used only under dynamic loading conditions, but not under static conditions. This study examined the distribution of stresses in a specimen by applying the principle of thermal elasticity. From the relationship between strength and stress, it was found that changes of temperature caused by measured stresses camera were consistent with the applied loads.

**Key Words:** Infrared(IR) Thermography, Thermal Stress, Nondestructive Testing(NDT), Fatigue Fracture, Lock-in

### 1. Introduction

Extensive studies have been conducted on the fatigue damage analysis for long time. Today's industries are faced with the needs to develop new products within a shorter period of time by shortening the design cycles. To fulfill such needs in the field of nondestructive testing, stress analysis methods using lock-in thermography are considered as a faster technology at the stage of design development.[1-4]

The recent significant progress in thermography technologies allowed developing equipment for non-contact full-field stress analysis.[5] A lock-in system contains a thermography camera, which measures the infrared emissions from the surface of a specimen under cyclic loading, and a lock-in module, which in real-time collects the loading signals of a fatigue tester from the thermography camera and noises and detects the detailed changes in temperature. Using a lock-in thermography system, this study examined the distribution of stresses in specimens by applying the principle of thermal elasticity.[6, 7] Further studies should be undertaken to resolve this limitation. Using a lock-in thermography system, this study examined the distribution of stresses in specimens by applying the principle of thermal elasticity.

### 2. Theoretical Background

Due to the first and second principles of thermodynamics, there is a relationship between temperature and mechanical behavior laws.[8] The relationship between thermal stress and strain in an isotropic, elastic element is given by

$$\Delta\varepsilon = \frac{(1 - 2\nu)\Delta\sigma}{E} + 3\alpha\Delta T \quad (1)$$

where,  $\Delta\varepsilon$  is the change of main strains summation,  $\Delta\sigma$  is the change of main strains summation,  $E$  is Young's modulus,  $\nu$  is Poisson's ratio,  $\alpha$  is linear dilatation coefficient, and  $\Delta T$  is difference of temperature.

When a force is applied to the specimen, the thermodynamic analysis of reversible and adiabatic behaviors of an elastic element is given by the linear thermo-elastic relation from Lord Kelvin equation(1850).

$$\Delta T = \frac{-3T\alpha K\Delta\varepsilon}{\rho C_v} \quad (2)$$

where,  $\Delta T$  is Temperature difference,  $T$  is absolute temperature,  $K$  is Bulk modulus,  $\rho$  is density, and  $C_v$  is the heat capacity at constant volume. Here,  $\Delta\varepsilon$  is the expansion of volume. If an element has no change in volume, the temperature will not change. Using the known relationship among the  $C_v$ , the thermal capacity under constant pressure, and the  $C_p$ , Equations (1) and (2) are combined to obtain an equation below describing the thermal elastic effects: Temperature changes is inversely proportional to the increase of stresses.

$$\Delta T = -\frac{\alpha}{\rho C_p} T \cdot (\sigma_1 + \sigma_2 + \sigma_3) \tag{3}$$

This relationship is effective only under an adiabatic condition. In the analysis of thermal elastic stresses,[9] the adiabatic condition can be obtained by applying cyclic stresses to a load-bearing member (>3Hz): the dynamic equilibrium (reversible condition) is maintained between the mechanical and thermal energies.

Equation (3) is a typical thermodynamic equation quantitatively describing the temperature change caused by the applied loads. The minus symbol indicates that the tension decreases the temperature while the compression increases the temperature. Under an adiabatic condition, the change in temperature will be proportional to the variation of the sum of the principal stresses. The thermal elastic modulus is given by

$$K_m = \frac{\alpha}{\rho C_p} \tag{4}$$

where  $K_m$  is the thermo-elastic coefficient. From materials engineering book, the typical  $K_m$  values of common engineering materials are shown in Table 1.

Table 1 Typical values of common engineering materials

Material	$\alpha$ (K <sup>-1</sup> ), 10 <sup>-5</sup>	$\rho$ (kg/m <sup>3</sup> )	$C_p$ (KJ/Kg K)	$K_m$ (MPa <sup>-1</sup> )
Steel	1.20	7800	400	3.14E-06
Cast iron	1.00	7800	500	3.56E-06
Titanium	8.55	4428	545	3.54E-06
Inox	1.20	7800	918	3.08E-06
Alu 42100	6.70	2735	441	2.67E-06
Iron	1.21	7870	1040	3.49E-06
Epoxy	3.50	1170	1700	2.88E-06
Polyester	8.00	1140	1700	4.13E-06
Alumina	7.70	3000	900	1.99E-06

### 3. Lock-in Thermography

This study used a thermography camera (made by CEDIP Infrared System; JADE 550M model) equipped with a two-dimensional Focal Plane Array (FPA) infrared detection device. Its resolution was 320 x 240 pixels, and the wavelength band was 3-5 μm. The infrared detection device used InSb or MCT and was cooled by a stirling cooler. The Noise Equivalent Temperature Differential (NETD) was 0.02°C at 30°C, which was the best among the commercial thermography cameras. As infrared stress analysis requires a better NETD level, 2,000 images were continuously collected and calculated at the frame rate of 100 Hz for 20 seconds using the lock-in method as shown in Figure 1.

Using the lock-in system at the frame rate at regular intervals, the thermographic data were continuously collected from specimens under cyclic loading and calculated to obtain the maximum temperature difference, ΔT, and then thermographic images. Contrast to conventional thermographic

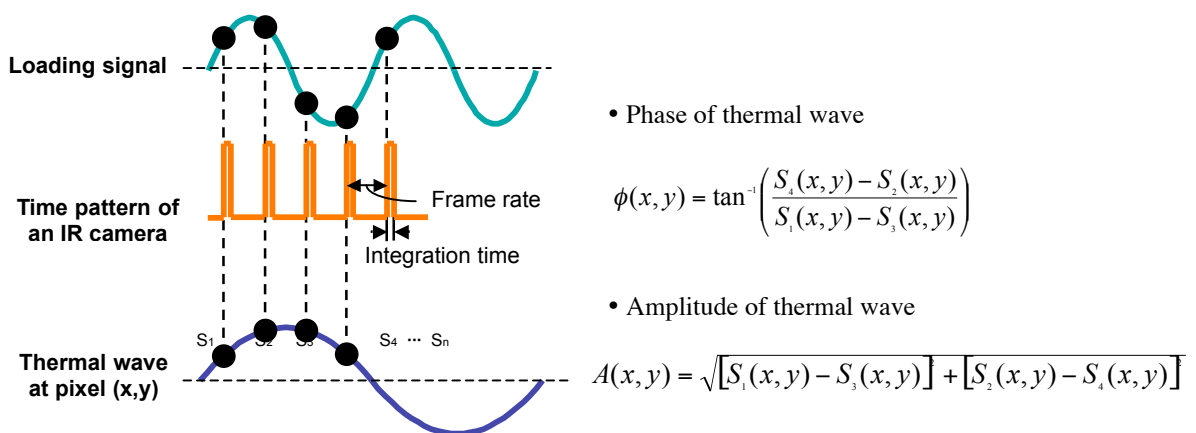


Fig. 1 Signal processing in Lock-in thermography

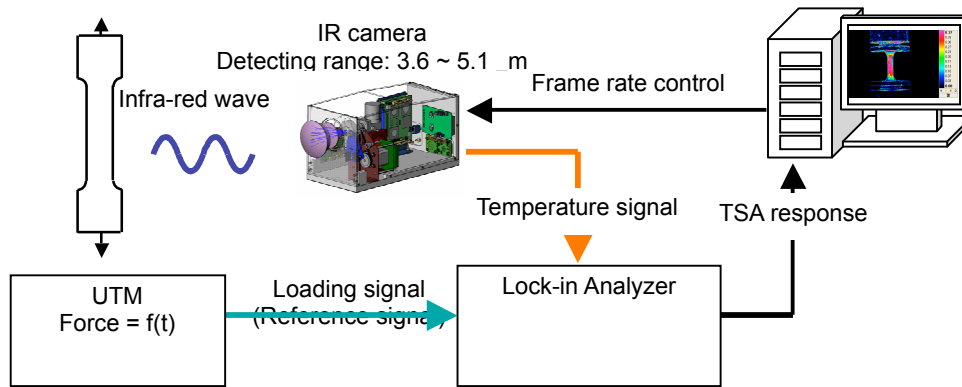


Fig. 2 Experimental set-up for Lock-in thermography

methods showing only the distribution of temperatures, this lock-in thermography combines the each phase of the loading signals from the fatigue tester with the temperature data from the thermography camera to calculate the thermographic data.

#### 4. Experiments

##### 4.1 Experimental set-up

As shown in figure 2, the specimen (FFC(T) SS400) was installed on the MTS fatigue tester to measure thermal stresses. To avoid any reflection from the specimen to the thermography camera, the specimen surface was sprayed for anti-reflection. The thermography camera was placed 1 meter in front of the installed specimen, and the lock-in module was set up so as to synchronize the loading signals from the fatigue tester and the temperature data from the IR thermography camera in real-time. To provide an adiabatic condition, heat sources were all removed from the laboratory.

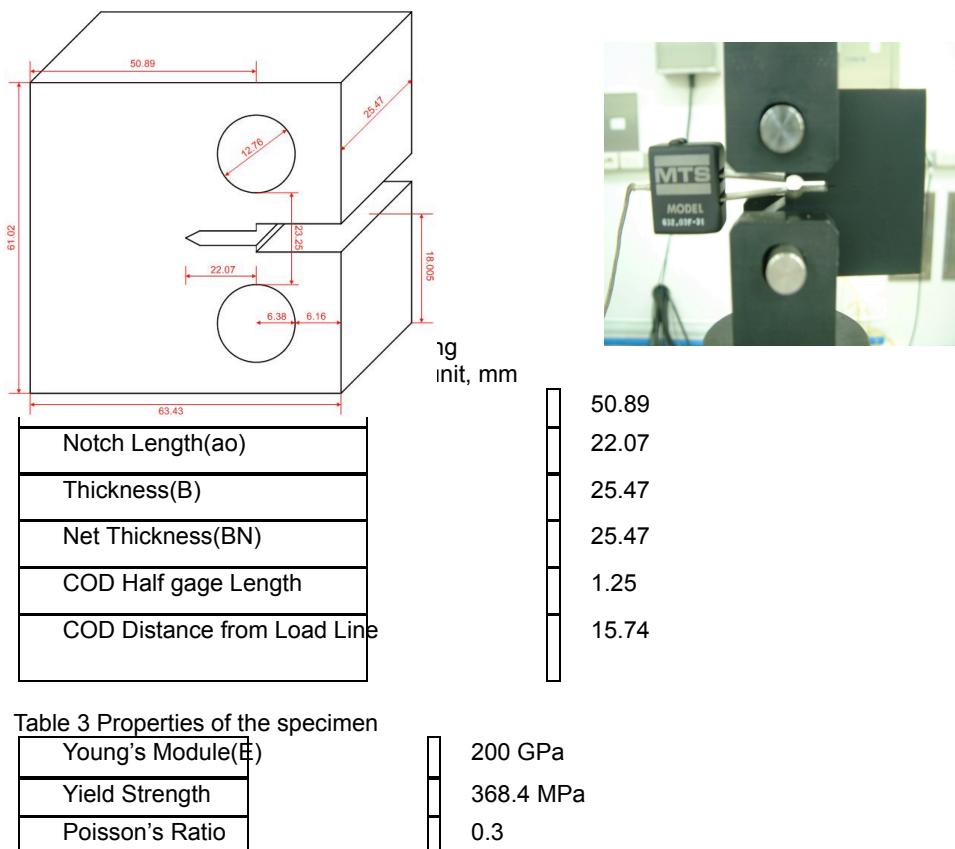
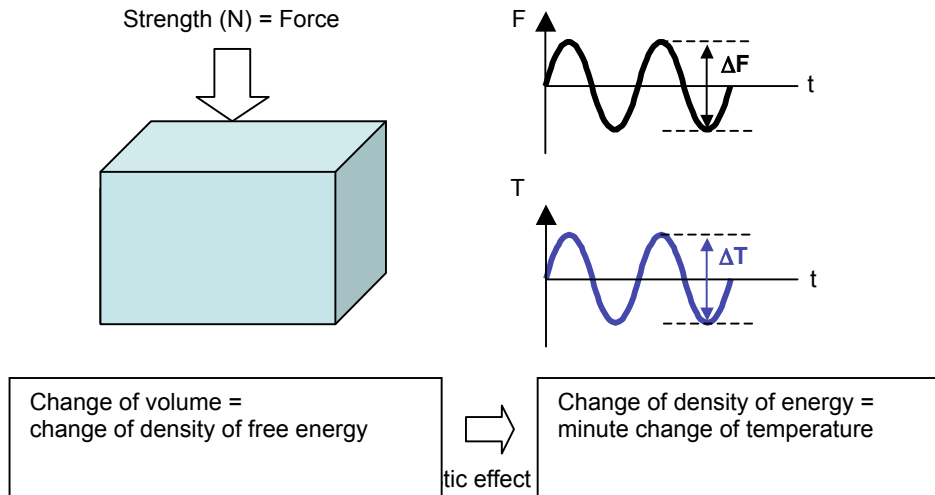


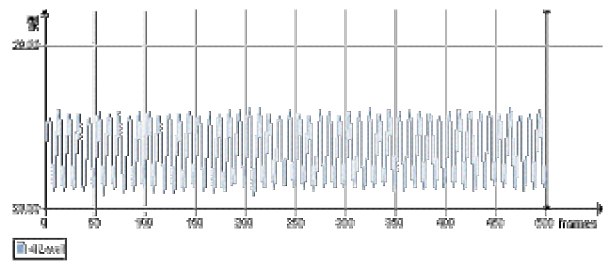
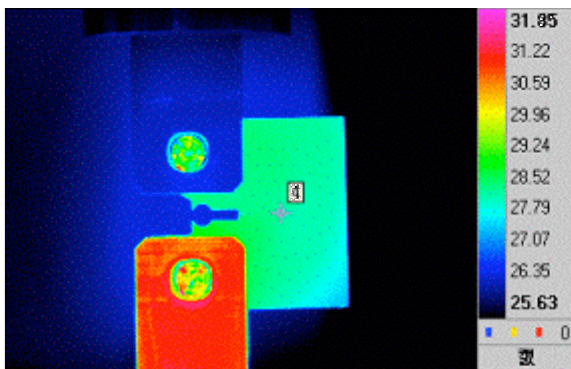
Figure 3 shows the FFC(T) as specimen and the photo mounted by installation to the MTS fatigue

tester. And, tables' 2 and 3 describes the geometry and properties, respectively

#### 4.2 Experimental Procedures

First of all the thermal elastic effects were examined: the changes in temperature were measured at the specimens under a constant load, and then the stress images taken by the IR thermography camera under cyclic stresses were analyzed. The relationship between the applied loads and stresses was also examined with actual tests. The IR thermographic images were taken by the thermography camera for 5 seconds at the rate of 100 images per second.





(a) Thermal patterns on specimen during dynamic  
(b) Temperature change at the spot with loading

max. temperature change

Fig. 5 Thermography imaging and temperature on loading

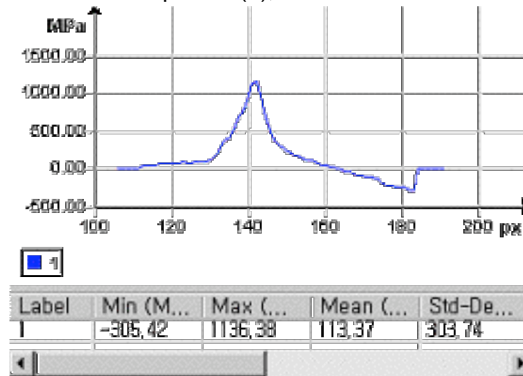
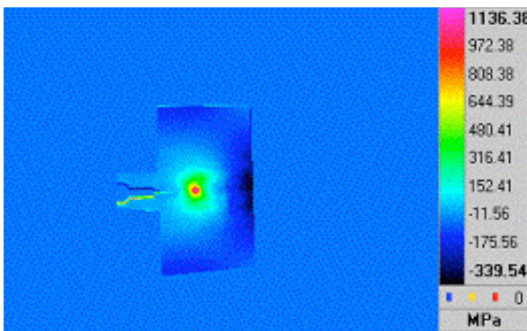
### 4.3 Stress Experiments

From figures 4, temperature changes due to the change of volume under loading conditions and total energy is constant. The biggest temperature difference was 0.50\_: the highest and lowest were 28.60\_ and 28.10\_, respectively. It was also found that the temperature decreased in tension and increased in compression in a cyclic pattern.

## 5. Results and Discussions

### 5.1. Stress Analysis

Figures 5 (b) show the changes in temperature when the fatigue tester is applied to cyclic loads in compression and tension, respectively. As the changes in temperature measured by the IR thermography camera are proportional to the principal stresses as described in Equation (3), the stresses can be



(a) Stress spot from thermal image applying elastic effect  
(b) stress map of the area showing stress concentration

Fig. 6 Stress spot and map in Lock-in thermography

px	139	140	141	142	143
130	557.61	582.43	586.75	569.82	499.91
131	615.78	653.06	674.27	659.57	587.45
132	682.24	753.41	805.14	800.77	712.74
133	761.59	871.04	976.30	987.92	858.97
134	829.60	961.93	1121.97	1136.38	966.91
135	796.00	929.12	1105.23	1117.82	942.23
136	713.05	823.61	932.97	940.49	818.88
137	637.97	709.27	756.36	754.65	684.32
	566.37	602.34	627.29	619.37	575.56
138	510.27	531.87	543.54	538.65	510.41

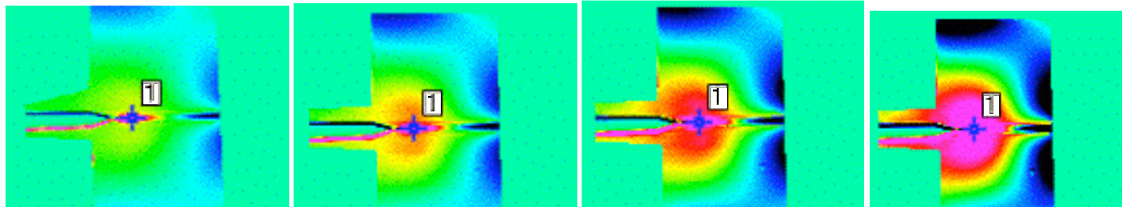
Fig. 7 Stress profile around the spot of maximum stress value

obtained by multiplying the temperature difference ( $\Delta T$ ) and the thermal elastic modulus ( $K_m$ ) of the material to show the stresses at all the pixels on a stress image as shown in figure 5. ~ 7 show a stress map and a stress profile zoomed-in at the stress-concentrated point, respectively. The stress-concentrated point was consistent with the expected one.

### 5. 2. Relation between loading condition and stress

In order to examine the relationship between the applied loads and stresses, a constant load was applied to the specimen at the interval of 10 Hz by increasing the load from 11 kN to 29 kN with an incremental of 6 kN to obtain the thermographic images at each load. The stress values (MPa) in the thermographic images were calculated by multiplying the temperature difference,  $\Delta T$ , in Equation (3) and the thermal elastic modulus,  $3.14 \times 10^{-6}$ , in Table 1.

As shown in Figure 9, analyzing each thermographic image for the maximum stress at the stress-concentrated point indicates that the stresses measured by the thermography camera are proportional to the applied loads. The analysis of the linear relationship between the strength and stress found in this study also implies that the changes in temperature caused by the measured stresses from the thermography camera were consistent with the applied loads.



(a) 343 MPa(11 KN) (b) 547 MPa(17 KN) (c) 763 MPa(23 KN) (d) 1010 MPa(29 KN)

Fig. 8 Thermo-elastic effect in Lock-in thermography

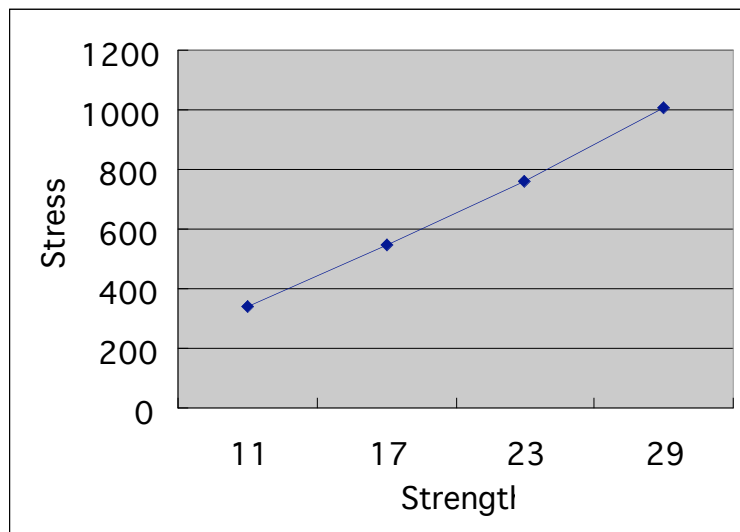


Fig. 9 Relationship between applied strength and stress

### 6. Conclusions and Remarks

The analysis of stresses in specimens using lock-in thermography was possible because the NETD levels of IR thermography cameras were dramatically improved. This technology can be used for the analysis of stresses or the prediction of fatigue limits in a non-destructive and non-contact way within a short time, so that users can obtain a stress map immediately from the nondestructive testing. As using this technology allows detecting any damaged or weak point, it is better than other conventional photo-elastic or ESPI methods.

Applying this thermographic measurement to fatigue testing would significantly reduce the necessary specimens and testing duration. As this technology is based on the thermal elastic effects, however, it can be used only under dynamic loading conditions, but not under static loading conditions. Further studies should be undertaken to resolve this limitation.

## References

1. D. Wu and G. Busse. Lock-in thermography for nondestructive evaluation of materials, *Rev. Gen. Therm.* 17 (1998) 693-703.
2. P. Bremond and P. Potet. Application of Lock-in thermography to the measurement of stress and to the determination of damage in material and structures, QIRT conferences (2000)
3. P. Bremond and P. Potet. Lock-in Thermography, A tool to analyze and locate thermo-mechanical mechnism in materials and structure, Thermosence XXIII April (2001)
4. M. P. Luong. Fatigue limit evaluation of metals using an infrared thermographic technique, *Mechanics of materials* 28 (1998) 155-163.
5. W. T. Kim, M. Y. Choi, Jung H. Park. Diagnosis of defect points in materials using infrared thermography, *Key Engineering Materials*, Vols. 297~300 (2005) 2169~2173.
6. J. H. Park, M. Y. Choi, W. T. Kim. Infrared thermography and modeling to the concrete deck with internal defects as a non-destructive testing, *Key Engineering Materials*, Vols. 270~273, (2004)
7. 98-1341. V. V. Pavlov. Thermal nondestructive testing: short history and state-of-art. In: Balageas D, Busse G, Carlomagno GM, editors *Proc. of the QIRT 1992, Eurotherm Series 27*. EETI ed., (1992) 179-93.
8. D. Wu, A. Salerno, B. Schonbach, H. Hallin, C. Busse. Phase-sensitive modulation thermography and its applications for NDE, *Proc. SPIE*, Vol. 3056, (1997) 176~182.